

## ARTICLE

# Hydrogen Adsorption Study upon Ni/Al<sub>2</sub>O<sub>3</sub> Nano-composite Synthesized by MOCVD Technique

Hameed Ullah<sup>a\*</sup>, Michael Veith<sup>b,c</sup>*a. Department of Chemistry, Hazara University Mansehra, KPK, Pakista**b. Institute for Inorganic Chemistry, Saarland University, Postfach 151150, 66041 Saarbruecken, Germany**c. INM-Leibniz Institute for New Materials, Campus D2 2, 66123 Saarbruecken, Germany*

(Dated: Received on January 19, 2013; Accepted on July 3, 2013)

The hydrogen adsorption (storage) studies upon Ni/Al<sub>2</sub>O<sub>3</sub> nano-composite prepared by metal organic chemical vapor deposition technique (MOCVD) exploiting single source molecular precursor (SSP) approach were carried out. The Ni/Al<sub>2</sub>O<sub>3</sub> nano-composite is prepared in cold walled MOCVD reactor by the decomposition of SSP, [H<sub>2</sub>Al(O<sup>t</sup>Bu)]<sub>2</sub>, on a substrate holding Ni(acac)<sub>2</sub> powder. The SSP is a reducing agent which reduces Ni<sup>+2</sup> to Ni<sup>0</sup> and works as source for Al<sub>2</sub>O<sub>3</sub> matrix in which the Ni<sup>0</sup> is dispersed. The resulting Ni/Al<sub>2</sub>O<sub>3</sub> nano-composite is characterized by XRD, SEM, TEM, and EDX. The hydrogen adsorption (storage) studies are performed using home-made Sievert's type apparatus. The hydrogen storage studies reveal that approximately 2.9% (mass ratio) hydrogen can be stored in the Ni/Al<sub>2</sub>O<sub>3</sub> nano-composite. The results show that Ni/Al<sub>2</sub>O<sub>3</sub> nano-composite can be a potential candidate for hydrogen storage which can be used for onboard fuel purposes.

**Key words:** Hydrogen, Ni/Al<sub>2</sub>O<sub>3</sub>, Nano-composite, Metal organic chemical vapor deposition technique, Adsorption

## I. INTRODUCTION

The human beings are facing the dangers of growing CO<sub>2</sub> emission (a main culprit of global warming) and the depleting fossil fuels resources, especially for onboard applications. To overcome these problems it is the need of the time to search alternative energy resources which could replace the fossil fuels and sustain the economic development and growth. Many alternative energy resources have been explored and exploited during the last few decades, *e.g.* solar energy, wind power, biomass, geothermal *etc.* However, these energy sources only provide few percent of the total global energy consumption [1]. Hydrogen as an alternative clean energy source has gotten attention during the last couple of decades due to its abundance and ecofriendly combustion [1]. Although, free hydrogen in the atmosphere is less than 1.0 ppm by volume but it is the 3rd most abundant element in the earth crust in binding form [2]. Besides, the ecofriendly combustion of hydrogen is its most attractive feature. The burning of hydrogen in presence of oxygen gives only water as byproduct beside energy: 2H<sub>2</sub>(g)+O<sub>2</sub>(g)→2H<sub>2</sub>O<sub>2</sub>(l)+Energy [3].

The transition from fossil fuels based economy into the hydrogen economy is governed by two main tech-

nical issues, the generation and storage of hydrogen. The current hydrogen generation methods are acceptable economically and environmentally. However, efficient and safe storage of hydrogen is the main hurdle in the transition.

Hydrogen can be stored in gaseous form by compressing into a tank, in liquid form by liquefying at cryogenic temperatures and solid form by adsorbing upon solid materials, *e.g.* metal hydrides. However, the gas and liquid modes of hydrogen storage have serious safety concerns, especially for onboard applications beside many other disadvantages [4]. The most efficient and safe form of hydrogen storage is the materials based with relatively large hydrogen contents per unit volume [5]. Therefore, a large number of materials have been investigated as hydrogen storage media [6–8]. One of the materials for solid hydrogen storage is the hydride, *e.g.* FeTiH<sub>2</sub>, LaNi<sub>5</sub>H<sub>6</sub>, MgH<sub>2</sub>, and alanates. However, hydrides are suffered as hydrogen storage materials by their slow adsorption and desorption kinetics which normally occurs at very high temperatures because of the chemisorption [9]. The discovery of highly porous materials, *e.g.* carbon nanotubes (CNTs) and metal organic frameworks (MOFs) paved the way for hydrogen storage in solid state at ambient conditions. Dillon *et al.* reported a significant amount (~10%) of hydrogen storage upon CNTs [10]. Yaghi *et al.* reported hydrogen storage upon MOFs [11]. Although some encouraging results have been reported, the materials studied so far

\* Author to whom correspondence should be addressed. E-mail: hameedwazir@yahoo.co.uk, FAX: +92-997-530046

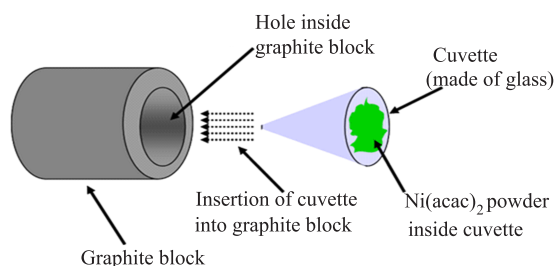


FIG. 1 Specially designed cuvette used for reduction of Ni(acac)<sub>2</sub> under flow of [H<sub>2</sub>Al(O<sup>t</sup>Bu)]<sub>2</sub>.

store hydrogen either by chemisorption which involves very high temperatures (>400 °C) adsorption/desorption kinetics or by physisorption which occurs at cryogenic temperatures. However, for practical onboard applications of hydrogen, the material should have the potential to reversibly store hydrogen in the pressure range of 1–10 bar and temperature range of 30–110 °C.

Here we report on hydrogen adsorption upon porous Ni/Al<sub>2</sub>O<sub>3</sub> nano-composite prepared by the *in situ* reduction of Ni(acac)<sub>2</sub> under the steady stream of single source molecular precursor (SSP), dihydridoaluminium tert-butoxide, in metal organic chemical vapor deposition technique (MOCVD) reactor. Approximately 2.9±0.2% hydrogen storage upon Ni/Al<sub>2</sub>O<sub>3</sub> nano-composite has been achieved.

## II. EXPERIMENTS

### A. General

The salts Ni(acac)<sub>2</sub>, LiAlH<sub>4</sub> and AlCl<sub>3</sub> were purchased from Sigma-Aldrich. The former two were used as received while the latter one was sublimed at 130 °C to ensure its high purity. All the solvents used were of analytical grade and dried well before use. The diethyl ether and benzene were distilled from sodium wires under nitrogen environment and stored over sodium wires. The alcohol and *t*-butanol were purified by distillation from magnesium turnings and stored over molecular sieves. The molecular SSP, [H<sub>2</sub>Al(O<sup>t</sup>Bu)]<sub>2</sub> was synthesized following a reported route and analysed by IR, <sup>1</sup>H NMR, and <sup>13</sup>C NMR spectroscopy and the results were matched with those reported in Ref.[12].

### B. Synthesis of Ni/Al<sub>2</sub>O<sub>3</sub> nano-composite

The material, Ni/Al<sub>2</sub>O<sub>3</sub> was synthesized according to the reported procedure [4]. Ni(acac)<sub>2</sub> was placed in a specially designed cuvette (Fig.1) and inserted into the CVD chamber. The design of CVD instrument is reported elsewhere [13]. The Ni(acac)<sub>2</sub> loaded CVD chamber was purged with gaseous nitrogen followed by inductive heating of the Ni(acac)<sub>2</sub> powder initially up to 250 °C. When the temperature stabilized,

the valve towards precursor was opened and its flow was directed over the cuvette for 10–15 min. Now the temperature was slowly raised to 580 °C and the precursor, [H<sub>2</sub>Al(O<sup>t</sup>Bu)]<sub>2</sub> flow was continued for another 15–20 min. When the process completed, the precursor flow was stopped by closing the valve and the heating was continued for another 5 min to ensure complete decomposition of the Ni(acac)<sub>2</sub> and precursor. After completion of the process, the heating was discontinued and the system was allowed to cool down to room temperature. The blackish Ni/Al<sub>2</sub>O<sub>3</sub> material was collected in clean ampoule and stored.

### C. Characterization of Ni/Al<sub>2</sub>O<sub>3</sub> nano-composite powder

XRD instrument (XPert-MPD Phillips using Cu Kα radiation) was used to analyse the phase, composition and structure of the Ni/Al<sub>2</sub>O<sub>3</sub> nano-composite. The XRD pattern corresponded to the earlier reported [4] and was indexed by corresponding to the PDF files. EDX spectrum was collected by EDX analyser connected to SEM (FEI Quanta 400 FEG). IR spectra were collected upon Varian 2000 FT-IR spectrophotometer.

### D. Hydrogen adsorption upon Ni/Al<sub>2</sub>O<sub>3</sub> nano-composite

The hydrogen adsorption upon Ni/Al<sub>2</sub>O<sub>3</sub> nano-composite was determined by using home-made Sievert's type apparatus. The detailed construction and function of the apparatus is reported elsewhere [14].

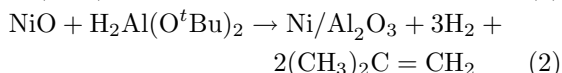
## III. RESULTS AND DISCUSSION

### A. Synthesis and characterization

Ni/Al<sub>2</sub>O<sub>3</sub> nano-composite was prepared by the *in situ* reduction of Ni(acac)<sub>2</sub> in a cold wall MOCVD reactor under the steady stream of SSP, [H<sub>2</sub>Al(O<sup>t</sup>Bu)]<sub>2</sub>. A specially designed cuvette was used for holding the Ni(acac)<sub>2</sub> powder inside the CVD reactor (Fig.1). The decomposition of Ni(acac)<sub>2</sub> under the steady stream of [H<sub>2</sub>Al(O<sup>t</sup>Bu)]<sub>2</sub> gave blackish powder of Ni/Al<sub>2</sub>O<sub>3</sub> nanocomposite. The resulting powder was stable in air and remained unreacted in open atmosphere for several months. It has been reported that the metallic nickel particles in nano range underwent a fast reaction with the atmospheric gases and got oxidized [15]. Therefore, the stability of nickel nanomaterials was one of the main issues. The lack of stability hindered the use of nickel nanomaterial and their storage for longer time under open atmosphere. But, the metallic nickel nanomaterials can be stabilized by making their composites or by dispersing in a matrix [16]. In the composite the atmospheric oxidizing agents are prevented by the matrix particles to reach the active nickel nanoparticles. The stability is more enhanced when the particles of the reinforcement (nickel) and matrix (Al<sub>2</sub>O<sub>3</sub>) are in nanometer level scale range. The enhanced stability is

due to the better grain boundary interaction among the particles of nickel and  $\text{Al}_2\text{O}_3$ . The greater stability of nickel nanoparticles has been achieved and successfully used as hydrogen storage medium.

The as-prepared  $\text{Ni}/\text{Al}_2\text{O}_3$  nano-composite powder was characterized by different techniques for its composition, structure and morphology. The powder XRD, SEM and TEM results have been reported in an earlier work [17]. The observed peaks in the XRD pattern corresponded to that of metallic nickel by matching with its PDF file. This indicates that the nickel is in zero oxidation state. The matrix material *i.e.*,  $\text{Al}_2\text{O}_3$  gave a broad peak which was the characteristic peak of amorphous alumina [18]. The XRD results showed that the material was obtained in two phases *i.e.*, the crystalline nickel phase and the amorphous alumina phase. Under normal conditions the precursor,  $[\text{H}_2\text{Al}(\text{O}^t\text{Bu})]_2$  undergo deposition in cold wall MOCVD reactor to give  $\text{Al}/\text{Al}_2\text{O}_3$  core shell nanocomposite in which the metallic aluminum is crystalline while the alumina is amorphous [18, 19]. The ratio of Al:O in the precursor is 1:1, while to get  $\text{Al}_2\text{O}_3$  the ratio must be 2:3. The extra oxygen required to get  $\text{Al}_2\text{O}_3$  comes from the  $\text{Ni}(\text{acac})_2$  which is reduced under the steady stream. It is thought that the  $\text{Ni}(\text{acac})_2$  underwent decomposition to give NiO at temperature  $>200^\circ\text{C}$  (Eq.(1)), which is subsequently reduced by the precursor to give  $\text{Ni}/\text{Al}_2\text{O}_3$  at temperature  $>500^\circ\text{C}$  (Eq.(2)).



No inhomogeneous strain was observed in the XRD pattern of  $\text{Ni}/\text{Al}_2\text{O}_3$  and thus the crystallite size,  $D$ , was estimated from peak width using the Scherrer's equation. The average crystallite size of the metallic nickel particles was estimated approximately 18 nm from XRD pattern of  $\text{Ni}/\text{Al}_2\text{O}_3$ . The amorphous nature of  $\text{Al}_2\text{O}_3$  hinders the particle size estimation by Scherrer's equation. However, the  $\text{Al}_2\text{O}_3$  particle size was estimated from the SEM micrographs.

The SEM micrographs obtained for the samples show the  $\text{Al}_2\text{O}_3$  nanoparticles in the range of 30–40 nm [17]. The same particle size of  $\text{Al}_2\text{O}_3$  was confirmed by TEM micrographs [17]. The metallic nickel nanoparticles are embedded in the  $\text{Al}_2\text{O}_3$  matrix and therefore, it is difficult to confirm the size from SEM micrographs. However, the TEM micrographs give a clear picture in which the metallic nickel nanoparticles dispersed in  $\text{Al}_2\text{O}_3$  matrix could be seen very clearly. The TEM micrographs confirm the particle size of the metallic nickel and the amorphous  $\text{Al}_2\text{O}_3$  estimated from XRD pattern and the SEM micrographs, respectively. The particle size of the crystalline metallic nickel and the amorphous  $\text{Al}_2\text{O}_3$  falls in the nanometer level scale (well below 100 nm). Therefore, the  $\text{Ni}/\text{Al}_2\text{O}_3$  material is thought to be pure nanocomposite.

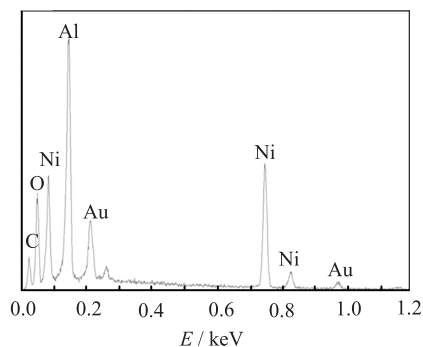
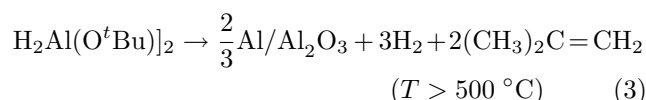


FIG. 2 EDX spectrum of  $\text{Ni}/\text{Al}_2\text{O}_3$  nano-composite.

The elemental composition of the  $\text{Ni}/\text{Al}_2\text{O}_3$  nanocomposite was established by EDX analysis. The EDX spectrum recorded for the  $\text{Ni}/\text{Al}_2\text{O}_3$  nano-composite shows nickel, aluminum and oxygen constituents of the material (Fig.2). The carbon peak in the EDX spectrum corresponds to the carbon tape used for adhesion of the powder upon the surface of sample stage. The sample was sputtered with gold to get better resolution of the SEM images and therefore, the gold peaks appear in the EDX spectrum of  $\text{Ni}/\text{Al}_2\text{O}_3$  nano-composite. The weight percent of Ni, Al and O in the  $\text{Ni}/\text{Al}_2\text{O}_3$  nanocomposite is estimated about 35.06, 36.27, and 28.67, respectively. The aluminum percentage is a little higher than stoichiometric amount of 33.59%. The overestimation of aluminum is due to the ability of precursor,  $[\text{H}_2\text{Al}(\text{O}^t\text{Bu})]_2$  to give  $\text{Al}/\text{Al}_2\text{O}_3$  upon decomposition. It is thought that the precursor is mainly utilized in reduction of  $\text{Ni}^{+2}$  to  $\text{Ni}^0$ . However, the unavailability of  $\text{Ni}^{+2}$  will lead to the previously reported natural decomposition of the precursor (Eq.(3)) [18, 19].



The natural decomposition of the precursor will result when the  $\text{Ni}^{+2}$  is completely reduced. The process needs an optimization to get stoichiometric  $\text{Ni}/\text{Al}_2\text{O}_3$  nanocomposite by controlling the flow rate and the deposition time of the precursor.

## B. Hydrogen adsorption upon $\text{Ni}/\text{Al}_2\text{O}_3$ nano-composite

Figure 3 shows the hydrogen adsorbed upon  $\text{Ni}/\text{Al}_2\text{O}_3$  nano-composite as a function of temperature. The amount of hydrogen adsorbed upon the  $\text{Ni}/\text{Al}_2\text{O}_3$  nano-composite is increasing with increasing temperature. The increase in hydrogen adsorption is comparatively sharp in the temperature range of 25–100  $^\circ\text{C}$  compared to the increase in hydrogen adsorption above 100  $^\circ\text{C}$ . The sharp increase in hydrogen adsorption in the temperature range of 25–100  $^\circ\text{C}$  corresponds to the

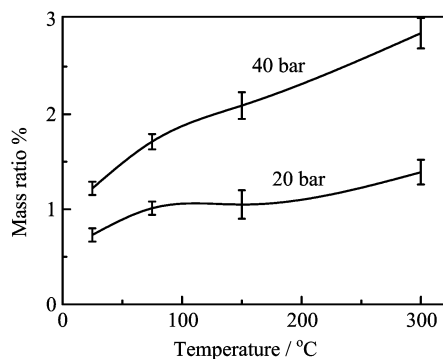


FIG. 3 Hydrogen adsorption as a function of temperature upon Ni/Al<sub>2</sub>O<sub>3</sub>.

physorption of hydrogen upon the Ni/Al<sub>2</sub>O<sub>3</sub>. We have observed and confirmed by DSC study in the case of Al/Al<sub>2</sub>O<sub>3</sub> core shell nanowires that the hydrogen adsorption predominantly occurs by physisorption mechanism in the temperature range of 25–100 °C [4]. The increase in hydrogen adsorption in this range is mainly due to the opening up of the structure as the temperature increases and ultimately more sites availability is made for hydrogen interaction which leads to increased amount of hydrogen adsorption [4]. Furthermore, at 20 bar (low pressure) and 40 bar (high pressure), the increase in hydrogen adsorption up to 100 °C is comparable. However, above 100 °C, the hydrogen adsorption is faster at high pressure than at low pressure. This may be due to increased reaction rate at high pressure than at lower pressure. The maximum amount  $2.9 \pm 0.2\%$  of hydrogen adsorption is shown at about 300 °C and 40 bar. From Fig.3, one can point out the effect of pressure upon the hydrogen adsorption. At constant temperature, the change in pressure significantly changes (increases) the amount of hydrogen adsorbed upon the Ni/Al<sub>2</sub>O<sub>3</sub> nanocomposite. At constant temperature of 300 °C, the hydrogen adsorbed upon the Ni/Al<sub>2</sub>O<sub>3</sub> nanocomposite increases by two fold, *i.e.* from  $1.4 \pm 0.2\%$  to  $2.9 \pm 0.2\%$  as the pressure increases from 20 bar to 40 bar.

To know the exact nature of hydrogen adsorption upon the Ni/Al<sub>2</sub>O<sub>3</sub> nanocomposite, IR spectroscopic analyses were performed upon the Ni/Al<sub>2</sub>O<sub>3</sub> nanocomposite before and after hydrogenation. Figure 4 shows the IR spectra of Ni/Al<sub>2</sub>O<sub>3</sub> nano-composite recorded before (1) and after hydrogen adsorption (2–8). The IR spectrum recorded upon the pre-hydrogenated sample gives three significant peaks at 3441, 2366, and 786 cm<sup>-1</sup> which are characteristics peaks of O–H, CO<sub>2</sub> and Al–O stretching vibrations, respectively. There is another peak which appears at 2366 cm<sup>-1</sup>. This peak is not because of any functional group but it is observed in all the spectra recorded with the IR machine available in our lab facility. This peak is because of inherited noise in the IR spectrophotometer. The spectra (2–6) are recorded for the samples

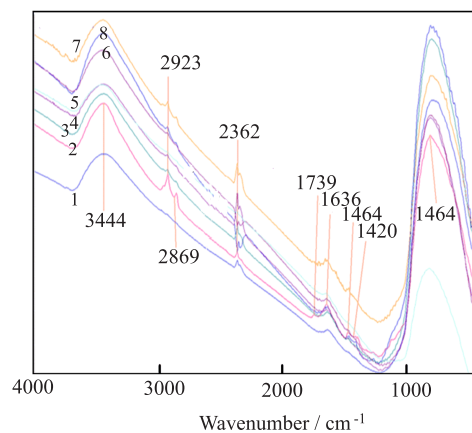


FIG. 4 IR spectra measured before and after hydrogen adsorption upon the Ni/Al<sub>2</sub>O<sub>3</sub> nano-composite at different temperatures (the different spectra are obtained: 1 before hydrogen adsorption; 2 at 25 °C and 40 bar, 3 at 75 °C and 20 bars; 4 at 75 °C and 40 bar, 5 at 150 °C and 20 bars, 6 at 150 °C and 40 bar, 7 at 300 °C and 40 bar, 8 at 300 °C and 20 bars.)

hydrogenated in the temperature range of 25–150 °C. It is very clear from the spectra (2–6) that no significant changes appear except for slight movement of the Al–O peak towards lower value and appearance of some less intense new peaks. However, the spectra (7) and (8) recorded for the samples hydrogenated at 40 and 20 bar, respectively at constant temperature of 300 °C show significant changes corresponding to the spectrum (1). These spectra show changes not only in the parent peaks but also some new peaks appear. The peaks due to Al–O and O–H stretching vibrations narrowed down compared to those of un-hydrogenated sample. The new peaks appearing at  $>3600$ , 2927, 1732, and 1459 cm<sup>-1</sup> could be assigned to O–H, C–H, and C=O stretching vibrations and C–H bending vibration, respectively. Although the peak at approximately 3600 cm<sup>-1</sup> is seen in all the spectra of Ni/Al<sub>2</sub>O<sub>3</sub> because of the free O–H group which is presented as inherited group but the peak is a bit intense in the case of sample (7) and (8). The relatively larger intensity of the peak in case of spectra (7) and (8) corresponds to the formation of free O–H groups as a result of chemical reaction between the hydrogen and the Ni/Al<sub>2</sub>O<sub>3</sub> nanocomposite. The same effect was observed in the hydrogenation of Al/Al<sub>2</sub>O<sub>3</sub> nanocomposite at temperature above 250 °C [4]. It was concluded that the hydrogen reacted chemically with the Al/Al<sub>2</sub>O<sub>3</sub> giving free O–H groups.

The hydrogen adsorption upon the Ni/Al<sub>2</sub>O<sub>3</sub> nanocomposite is purely governed by the chemisorption mechanism which is evident from the increasing amount of hydrogen adsorption with increasing temperature. However, at low temperature the physisorption could not be ruled out. As the temperature increases the structure of material opens up and the hydrogen

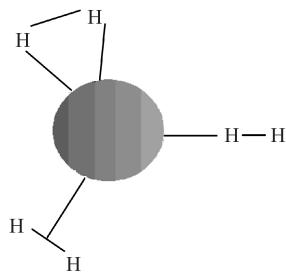


FIG. 5 Different possible modes of  $H_2$  interaction with the particles of  $Ni/Al_2O_3$ .

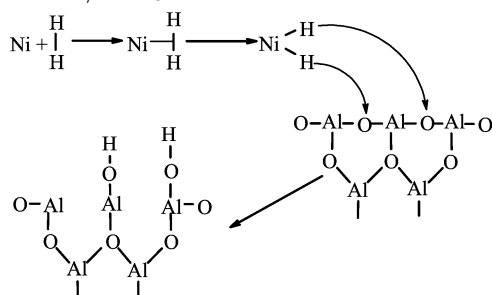


FIG. 6 Schematic representation of  $Al_2O_3$  network rupturing at  $300\text{ }^\circ\text{C}$ .

molecules have better access to the active sites of the material and thus more reaction possibilities [14]. However, at low temperature the dissociation of hydrogen molecule is not the favorite reaction which is evident from the IR spectra in the temperature range of  $25\text{--}150\text{ }^\circ\text{C}$  where no new peaks appear (Fig.4). Therefore, it is thought that the hydrogen acts as ligand and reacts with the material as ligand while retaining its molecular form. The different possibilities of molecular hydrogen bonded with the  $Ni/Al_2O_3$  material as ligand are pictorially shown in Fig.5. The possibilities of hydrogen working as ligand while retaining its molecular form are also reported and determined by inelastic neutron diffraction in case of other materials [20]. However, at high temperature ( $300\text{ }^\circ\text{C}$ ) the dissociation of hydrogen molecule is evident. In the IR spectra (7 and 8) the increase in intensity of the peaks appears above  $3600\text{ cm}^{-1}$  correspond to O–H (free) stretching vibration. These free O–H groups could be formed by the reaction of  $H_2$  with the  $Al_2O_3$  network and consequently the network ruptured to give O–H groups (Fig.6). Previously it has been reported that the Ni catalyzed the reaction by breaking  $H_2$  molecule into hydrogen radicals which then shift to the  $Al_2O_3$  network and rupture it [21].

#### IV. CONCLUSION

Hydrogen adsorption upon  $Ni/Al_2O_3$  nano-composite has been studied using home-made Sievert's type apparatus. Approximately,  $2.9\pm 0.2\%$  hydrogen storage upon  $Ni/Al_2O_3$  nano-composite have been achieved. The pre- and post-hydrogen adsorption analysis of the

material revealed that the adsorption of hydrogen upon the  $Ni/Al_2O_3$  nano-composite occurred by chemisorption mechanism at temperature above  $100\text{ }^\circ\text{C}$ . However, at temperature below  $100\text{ }^\circ\text{C}$  physisorption could not be ruled out. In the temperature range of  $25\text{--}150\text{ }^\circ\text{C}$ , the hydrogen reacted with the material as ligand and retained its molecular nature. However, as temperature reached  $300\text{ }^\circ\text{C}$ , the chemisorption involved the splitting of molecular hydrogen into atomic hydrogen which then reacted with the alumina network and ruptured it to give free O–H groups. It is pertinent to mention here that the hydrogen desorption study of  $Ni/Al_2O_3$  nanocomposite is under progress. Furthermore, the theoretical studies to know the nature of hydrogen adsorption upon the  $Ni/Al_2O_3$  nanocomposite will be conducted.

- [1] Z. X. Guo, C. Shang, and K. F. Aguey-Zinsou, *J. Europ. Cer. Soc.* **28**, 1467 (2008).
- [2] M. Dresselhaus, G. Crabtree, M. Buchanan, T. Mallouk, K. Taylor, P. Jena, F. DiSalvo, T. Zawodzinski, and H. Kung, *Basic Research Needs for the Hydrogen Economy*, Chicago, USA: Argonne National Laboratory (2003).
- [3] J. Rifkin, *The Hydrogen Economy*, 1st Edn. New York, USA: Tarcher, (2002).
- [4] H. Ullah, *Ph. D Dissertation*, Saarbruecken: Saarland University, Germany (2010).
- [5] L. Schalpbach, *Mater. Res. Sci. Bull.* **27**, 675 (2002).
- [6] X. B. Wu, P. Chen, J. Lin, and K. L. Tan, *Int. J. Hydrogen Energy* **25**, 261 (2000).
- [7] C. X. Shang and Z. X. Guo, *J. Power Sources* **129**, 73 (2004).
- [8] Z. S. Wronski, *Int. Mater. Rev.* **46**, 1 (2001).
- [9] R. Checchetto, G. Trettel, and A. Miotello, *Meas. Sci. Technol.* **15**, 127 (2004).
- [10] A. C. Dillon, K. M. Jones, T. A. Bekkedahl, C. H. Kiang, D. S. Bethune, and M. J. Heben, *Nature* **386**, 377 (1997).
- [11] N. L. Rosi, J. Eckert, M. Eddaoudi, D. T. Vodak, J. Kim, M. O'Keeffe, and O. Yaghi, *Science* **300**, 1127 (2003).
- [12] M. Veith, S. Faber, H. Wolfanger, and V. Huch, *Chem. Ber.* **129**, 381 (1996).
- [13] M. Veith and S. Kneip, *J. Mater. Sci. Lett.* **13**, 335 (1994).
- [14] H. U. Wazir, *Ligand-Modified Metal Alkoxides: The Chemistry and Applications*, 1st Edn., Saarbruecken: VDM Verlag, (2010).
- [15] M. C. B. Bradford and M. A. Vannice, *Catal. Rev. Sci. Eng.* **41**, 1 (1999).
- [16] D. Vanoppen, M. Veith, and K. Valtchev, United States Patents, No.US7026269B2 (2006).
- [17] H. Ullah, *Adv. Mater. Res.* (in press) (2013).
- [18] M. Veith, E. Sow, U. Werner, C. Petersen, and O. C. Aktas, *Eur. J. Inorg. Chem.* 5181 (2008).
- [19] M. Veith, S. Faber, R. Hempelmann, S. Janssen, J. Prewo, and H. Eckerlebe, *J. Mater. Sci.* **31**, 2009 (1996).
- [20] B. L. Mojet, J. Eckert, R. A. van Santen, A. Albinati, and R. E. Lechner, *J. Am. Chem. Soc.* **123**, 8147 (2001).
- [21] K. Iyakutti, Y. Kawazoe, M. Rajarajeswari, and V. J. Surya, *Int. J. Hydrogen Energy* **34**, 370 (2009).